[AMERICAN JOURNAL OF SCIENCE, VOL. 297, OCTOBER, 1997, P. 807–828]

PYRRHOTITE LEACHING IN ACID MIXTURES OF HCl AND H_2SO_4

ALLEN R. PRATT* and H. WAYNE NESBITT
Department of Earth Science, University of Western Ontario, London, Ontario, Canada, N6A 5B7

ABSTRACT. Pyrrhotite (Fe_7S_8) was leached in air-equilibrated pH 3.0 HCl H_2SO_4 acid mixtures with Cl^-:SO_4^{2-} ratios of 1:0, 3:1, 1:1, 1:3 and 0:1. AES depth profiles and XPS analyses of reacted surfaces were consistent with several compositional layers including a surface coating of Fe(III)-oxyhydroxide, an underlying zone of sulfur enrichment which decreased in sulfur content with depth, and finally unaltered pyrrhotite. Leaching experiments showed that iron concentrations increased linearly in solution as a function of the square-root of time. This relationship was indicative of a diffusion-limited reaction. Sulfate concentrations increased rapidly to 1.0 ppm within the first few minutes of reaction, then remained unchanged over the duration of the experiment. These results demonstrate that sulfate release was a rapid one-time event in the earliest stages of pyrrhotite dissolution.

Pyrrhotite leaching in acid solutions proceeded via the diffusion of iron to the mineral surface. With the removal of iron from the pyrrhotite structure, polysulfide replaced monosulfide as the dominant sulfur species. The Fe(III)-oxyhydroxide was determined to be the product of reaction between oxygen and iron species at the surface. Pyrrhotite surfaces reacted in solutions containing the greater sulfate concentrations were found to have the thickest Fe(III)-oxyhydroxide layers. In contrast, surfaces reacted with solutions containing appreciable chloride developed sulfur-rich near surfaces with an overlying thin veneer of Fe(III)-oxyhydroxide. Results of the study suggest that chloride inhibited the formation of surface Fe(III)-oxyhydroxides and promoted the development of sulfur-rich sublayers. Cl^-:SO_4^{2-} ratios in solution did not appear to have any significant effect on leach rates of iron.

INTRODUCTION

Pyrrhotite is a particularly reactive sulfide mineral, and during its oxidation and dissolution it can contribute significantly to the increased acidity and metal content of fluids seeping from sulfide-bearing mine wastes. Although pyrrhotite is a major gangue mineral of many ore deposits, its weathering characteristics are not well documented, nor are the nature of reactions occurring at the mineral fluid interface well understood.

The dissolution of pyrrhotite is known to proceed incongruently, and the process is characterized by preferrential release of iron relative to sulfur (Ahonen and Tuovinen, 1992; Bhatti and others, 1993; Nicholson and Scharer, 1994). Within actual sulfide mine tailing settings pyrrhotite grains have been observed to develop alteration rims enriched in sulfur (Blowes and Jambor, 1990).

* Present address: Surface Science Western University of Western Ontario London, Ontario, Canada, N6A 5B7

Fluids seeping from sulfide mine wastes contain elevated amounts of dissolved cations and anions. Two common anions in waters associated with sulfide mine waste storage areas are sulfate and chloride (Hutchinson and Elles, 1992; Caboi and others, 1992). Sulfate generally constitutes a much greater component of mine tailing pore water than does chloride (Ritcey, 1989; Blowes and Jambor, 1990), but chloride concentrations of some drainage waters approach and even exceed sulfate concentrations (Tones, 1982, p. 37; Ritcey, 1989, p. 226; Hutchinson and Elles, 1992, p. 629; Caboi and others, 1992, p. 369; Al and others, 1994, p. 339). Concentration profiles in waters of waste dumps demonstrate that sulfate is dramatically decreased near redox boundaries, and molar ratios of chloride to sulfate approach or even exceed unity. The purpose of this study is to investigate the effects that chloride and sulfate have on the mineral surface chemistry and dissolution rate of pyrrhotite.

Buckley and Woods (1985a,b) and Jones and others (1992) summarized previous surface studies of pyrrhotite. Buckley and Woods (1985a) report that pyrrhotite reacted in acetic acid (pH $\approx$ 2.4) developed iron-depleted surfaces. Maximum peak intensities for Fe($2p_{3/2}$) spectra were reported to occur at 707.5 eV. Their S($2p$) spectra indicate sulfur is present mainly as polysulfide species with binding energies slightly lower than elemental sulfur. They suggested that a soluble iron(II) species had formed under these conditions and that the near-surface may be restructured to form an iron polysulfide rather than a sulfide within the stoichiometry range of pyrrhotite. Jones and others (1992) reacted pyrrhotite in perchloric acid (pH $\approx$ 1.3) and obtained similar results. In addition, Jones and others (1992) provide structural evidence that the polymerized sulfur atoms occur in linear chains with S-S distances comparable to elemental sulfur.

Pyrrhotite leached in sulfuric acid (pH = 3.0) were found to have near-surfaces which were compositionally stratified (Pratt, Nesbitt, and Muir, 1994). The outermost layer was observed to be an iron(III)-oxyhydroxide of varying thickness (80Å to >500Å). Separating the surface iron(III)-oxyhydroxide and the underlying unaltered pyrrhotite was a sulfur-rich zone. Within this zone no oxygen species were detected, and sulfur was present mainly as polysulfides.

METHODS

Materials and experiments.–Two sets of experiments were conducted. The first investigates the mineral chemistry of pyrrhotite surfaces leached by HCl and H_2SO_4 mixtures, pH 3.0, containing Cl^-:SO_4^{2-} mole ratios of 1:0, 3:1, 1:1 and 1:3 (all subsequent numeric anion ratios cited refer to the mol ratio of Cl^- to SO_4^{2-}. Pyrrhotite surfaces were analyzed with Auger electron spectroscopy (AES) and X-ray photoelectron spectroscopy (XPS). XPS provided chemical state information, and AES compositional information. Comprehensive introductions to XPS and AES are presented in Hochella (1988). The second set of experiments examines pyrrhotite leaching rates using the same acid mixtures (3:1, 1:1, 1:3) and an additional solution of H_2SO_4 only (0:1).

Euhedral pyrrhotites (Fe_7S_8) from Chihuahua, Mexico were used for the analytical experiments and have been described elsewhere (Pratt, Muir, and Nesbitt, 1994). Massive pyrrhotite from the Kidd Creek Mine, Canada was used in the dissolution batch experiments. The pyrrhotite from both localities was the monoclinic variety with a minor hexagonal component.

Pyrrhotite laths 3 to 5 mm long and 2 to 3 mm in cross section were prepared, fractured, and reacted in 80 mL of air-equilibrated solutions of pH 3.0 at 20°C ± 1°C. Separate experiments were conducted for each of the $Cl:SO_4$ ratios indicated above. Following 8 hrs of reaction, specimens were removed from the solutions and passively dried in a nitrogen environment at room temperature for 12 to 16 hrs. All pyrrhotite manipulations prior and

TABLE 1

XPS reference binding energies for chemical species. All values in eV

Species	Binding Energy	Source
Fe($2p_{3/2}$)		
Fe(II)-S	706.7	Van der Heide and others (1980)
	707.0	Nesbitt and Muir (1994)
	707.45	Pratt, Muir, and Nesbitt (1994)
	707.5	Jones and others (1992)
Fe(III)-S	709.2	Pratt, Muir and Nesbitt (1994)
FeO	709.5†	McIntyre and Zetaruk (1977)
	709.6*	Mills and Sullivan (1983)
Fe_3O_4	708.3†	Fe^{2+}-McIntyre and Zetaruk (1977)
	710.8†	Fe^{3+}-McIntyre and Zetaruk (1977)
	710.8*	Mills and Sullivan (1983)
αFe_2O_3	711.0†	McIntyre and Zetaruk (1977)
	711.0*	Harvey and Linton (1981)
	711.0†	Junta-Rosso and Hochella (1996)
αFeOOH	711.6†	McIntyre and Zetaruk (1977)
	711.6*	Harvey and Linton (1981)
S(2p)		
S^{2-}	161.1	Buckley and Woods (1985b)
	161.3	Pratt, Muir, and Nesbitt (1994)
S_2^{2-}	162.5	Nesbitt and Muir (1994)
S_n^{2-}	163.7	Hyland and Bancroft (1989)
S_8	163.8	Wagner and others (1979)
	164.2	Carlson (1975)
SO_4^{2-}	168.5	Jones and others (1992)
O(1s)		
αFe_2O_3 oxide	529.8	McIntyre and Zetaruk (1977)
	530.0	Junta-Rosso and Hochella (1996)
hydroxide	531.4	Mills and Sullivan (1983)
αFeOOH oxide	530.0	Ferris and others (1989)
	530.3	McIntyre and Zetaruk (1977)
hydroxide	530.9	Harvey and Linton (1981)
	531.4	McIntyre and Zetaruk (1977)
physically adsorbed H_2O	532.3	Harvey and Linton (1981)
	533.5	Knipe and others (1995)
	533.8	Jones and others (1992)

*: Measurement taken at peak maximum.
† : Center of gravity measurement.

subsequent to acid reaction were conducted in nitrogen or argon gas filled chambers to minimize contamination by atmospheric gases.

The Kidd Creek pyrrhotite was crushed dry in air and screened to provide −250 μm +125 μm mesh fractions for the batch leaching studies. Crushed samples were used within 24 hrs of preparation. Experiments were carried out at 25° and 35°C (±0.1°C). To each 200 mL acid mixture was added 5 g of crushed and seived pyrrhotite. The mixtures were agitated with a Teflon stirrer at 600 rpm. To minimize evaporation effects, the beakers were covered with parafilm. Filtered (0.2 μm mesh) aliquots were drawn at regular intervals over 24 to 30 hrs and analyzed for pH, total iron, ferric iron and sulfate.

Instrumentation and data analysis.–XPS analyses were carried out with a Surface Science Laboratories SSX-100 X-ray photoelectron spectrometer equipped with a monochromatized Al Kα X-ray source (spot size 300-600 μm) and a base pressure of 2×10^{-9} Torr. The spectrometer was calibrated to the Au($4f_{7/2}$) line at 84.00 eV and to give an energy difference of 857.1 eV between the metallic copper $3p_{3/2}$ and $2p_{3/2}$ lines. The analyzer pass energy was 25 eV. High resolution spectra were analyzed using a Shirley background (Shirley, 1972) and a Gaussian-Lorentzian peak fit model. With these calibrations, the acid leached pyrrhotite specimens had an Fe($2p_{3/2}$) (Fe(II) sulfide peak) binding energy of 707.4 ± 0.05 eV and a S($2p_{3/2}$) monosulfide peak binding energy of 161.4 ± 0.05 eV. No charge correction was necessary, based on Fe($2p_{3/2}$) and S($2p$) peak positions and the reproducibility of sample binding energies. Iron, sulfur, and oxygen species binding energies listed in table 1 were used as references for spectra peak fitting. To minimize the number of Fe($2p_{3/2}$) freely adjustable peak parameters, ferrous and ferric contributions were fit by strictly adhering to the detailed Fe($2p_{3/2}$) fitting procedures presented by Pratt, Muir, and Nesbitt (1994) and Nesbitt and Muir (1994). S($2p$) peaks were fit with spin orbit doublet S($2p_{3/2}$) and S($2p_{1/2}$) lines. The S($2p_{1/2}$) line was constrained to precisely half the area of and to 1.18 eV higher energy than the S($2p_{3/2}$) line.

AES data were acquired using a Perkin-Elmer Phi 600 scanning Auger microprobe equipped with a secondary electron detector and an Ar^+ ion gun. During sputtering, base pressure of the analytical chamber was approx 3×10^{-8} Torr. Analyses were obtained using a 3 kV, 20 nA electron beam focused to a 3 μm spot size. Depth profiles were collected by rastering a near 30° incident 2.0 kV Ar^+ beam over a 2 × 2 mm surface. Approximate sputter rates under these conditions were 40Å min^{-1} ± 10 percent for pyrrhotite (Pratt, Muir, and Nesbitt, 1994) and 40Å min^{-1} ± 20 percent for ferric oxide (Physical Electronics, 1976). Atomic compositions were calculated following the procedures and guidelines presented by Nesbitt and Pratt (1995).

The concentration of iron in the solutions was measured using atomic adsorption (AA) (±0.2 mg/L). Ferric iron concentrations were determined using the colorimetric ammonium thiocyanate method (Sandell, 1959, p. 522-535). The limit of detection was found to be 50 μg/L (±10 μg/L). Sulfate concentrations in the 25°C 1:0 acid mixture were determined by ion chromatography (IC) (±0.1 mg/l).

RESULTS

Secondary electron images showed that the leached pyrrhotite surfaces were topographically smooth and devoid of recognizable features on the scale of 0.2 μm. XPS and AES survey scans detected no chloride on analyzed surfaces (fig. 1). Representative high resolution XPS spectra of acid leached surfaces are shown in figure 2. Peak fitting results are listed in tables 2, 3 and 4. Typical Auger depth profiles are shown in figure 3. Surfaces were monitored periodically during depth profile collection for electron beam induced surface modifications. None was observed. The intensity of the C KLL signal decreased to that of background following one cycle of sputtering, indicating it was an adventitious contaminate.

Concentrations for iron, sulfate, and pH obtained from batch experiments are presented in figures 4 and 5. Iron and sulfate concentrations have been corrected for the amount of solution removed for analysis. Experimental leach rate constants are listed in table 5. Surface areas were estimated by assuming grains in the screened −250 μm +125 μm mesh fractions had largely spherical shapes and average diameters of 187 μm. Fe(III):Fe(II) mole ratios were observed to be near 0.01 over the duration of the experiments. For all the batch leaching runs a barely detectable (undetectable by some people) H_2S odor was noticed. After approx 20 hrs of reaction at 25°C and 6 hrs of reaction at 35°C a yellow-to-rust colored colloidal suspension was observed in the leaching solutions. XRD analysis show the suspensions were lepidochrosite (γFeOOH) with lesser amounts of elemental sulfur (S^0).

INTERPRETATION

XPS spectra.–The $Fe(2p_{3/2})$ spectra collected from leached pyrrhotite (fig. 2A) surfaces are characterized by peaks near 707 and 711 eV. The $Fe(2p_{3/2})$ spectra are fit with multiplet splitting magnitudes and intensities for the free ferrous and ferric ions calculated from theory by Gupta and Sen (1974, 1975). For transition metals, multiplet splitting results from interaction of unpaired $3d$ electrons with core level 3p electrons of like-spin during a photoelectron event (Hochella, 1988). Detailed discussions and procedures on the curve fitting of Fe(2p) spectra are presented in Pratt, Nesbitt, and Muir (1994), Pratt, Muir, and Nesbitt (1994), and Nesbitt and Muir (1994).

The primary Fe(II)-S peak is fit at 707.4 eV, and the two multiplets are at 0.95 eV higher and lower binding energies, as required by theory (fig. 2; table 2; Pratt, Muir, and Nesbitt, 1994; McIntyre and Zetaruk, 1977; Gupta and Sen, 1974, 1975). The intensities of the three peaks are adjusted to obtain the best fit. The intensity of the higher binding energy multiplet peak is consistently five times greater than the intensity of the lower binding energy multiplet (fig. 2). This 5:1 intensity ratio is more characteristic of pyrite (Nesbitt and Muir, 1994) than of pristine pyrrhotite, where the ratio is close to 1:1 (Pratt, Muir, and Nesbitt, 1994). This peak modelling result may indicate that the surface restructured to the disordered pyrite seen by Jones and others (1992) on pyrrhotite surfaces reacted in perchloric acid.

The broad asymmetric peak near 711.0 eV spans the range of binding energies reported for iron(III) oxides and hydroxides (table 1). Following the

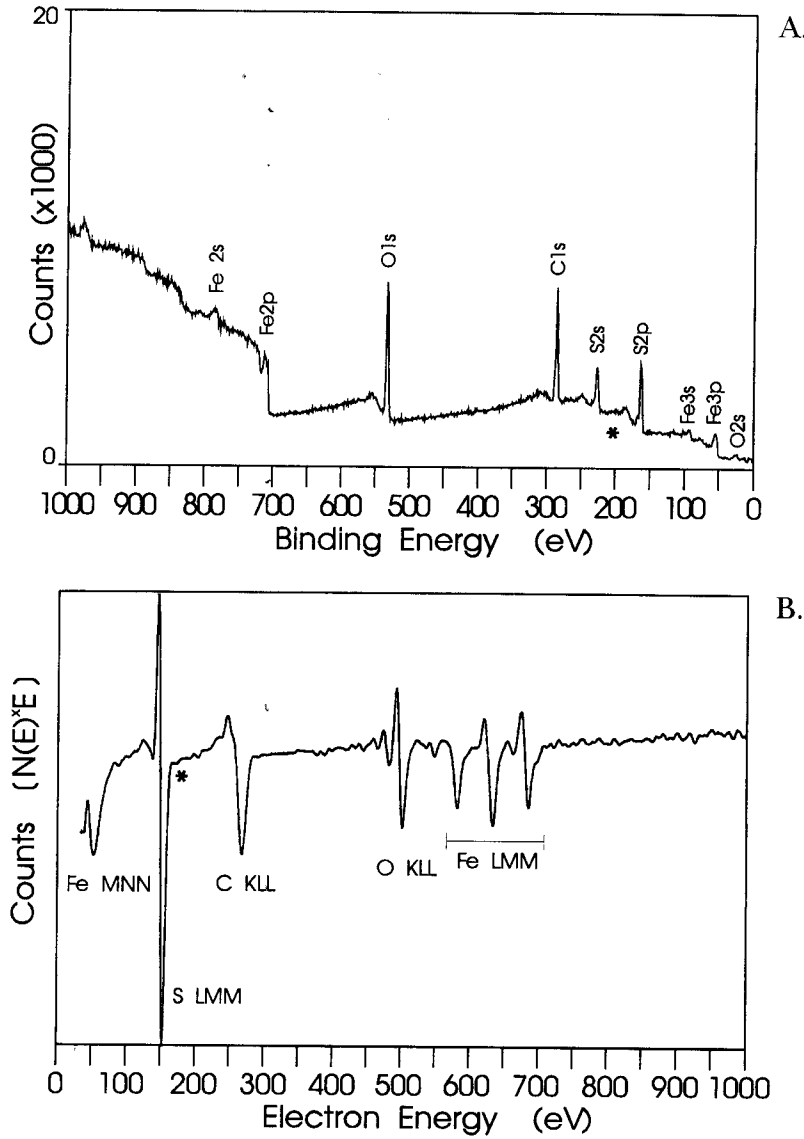

Fig. 1. XPS survey scan of a Cl^-:SO_4^{2-} 3:1 leached pyrrhotite surface (A) and AES survey scan of a Cl^-:SO_4^{2-} 1:3 reacted pyrrhotite surface (B). Elements detected are sulfur, iron, oxygen and carbon. Asterisks mark the approximate position of primary chloride peaks. The high background of the XPS spectrum at binding energy above 800 eV is due to inelastically scattered electrons.

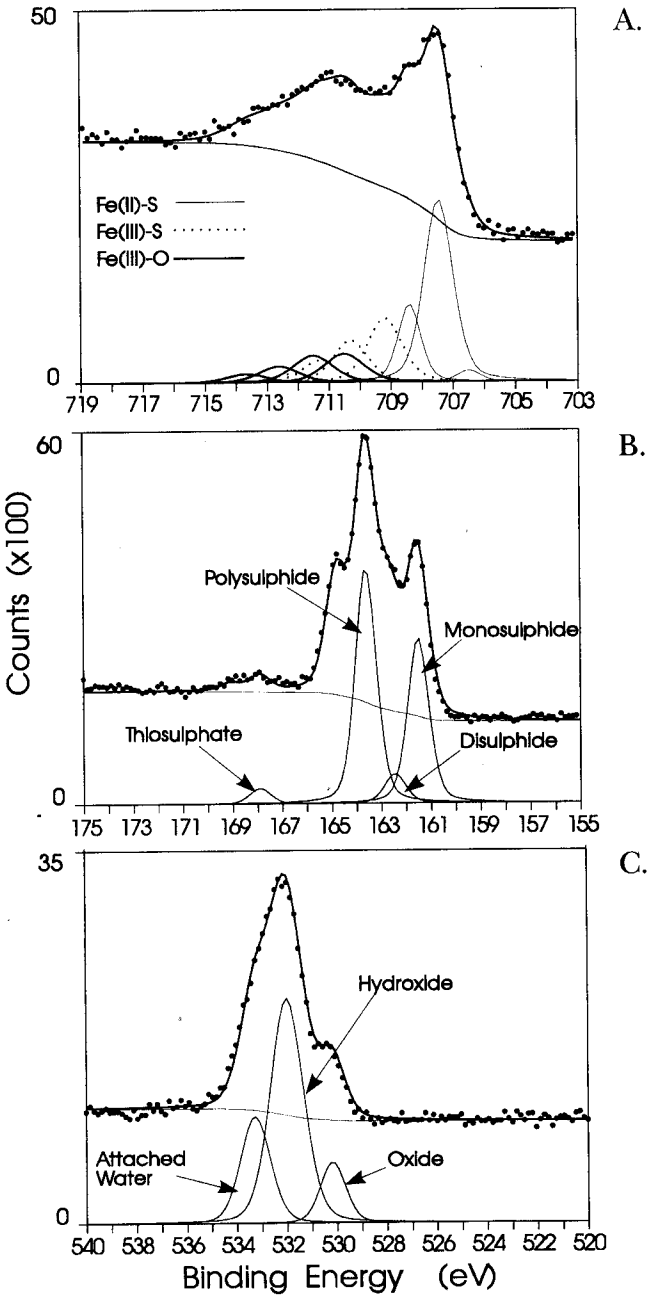

Fig. 2. Representative XPS high resolution narrow region scans collected from Cl^-:SO_4^{2-} 1:1 acid reacted pyrrhotite surfaces: (A) Fe($2p_{3/2}$); (B) S($2p$); (C) O($1s$). XPS peak fitting details for pyrrhotite leached in the various acid mixtures are presented in tables 2, 3 and 4.

TABLE 2

Fe(2$p_{3/2}$) peak fitting data, energies listed refer to the primary Fe(II) and the lowest energy Fe(III) multiplet peaks. See note below for position and intensity of subsequent multiplet peaks. The FWHM for the main Fe(II)-S peak is 1.1 eV and the multiplets 0.9 eV. FWHM for Fe(III)-S peaks are 1.3 eV, and Fe(III)-O peaks are 1.5 eV

Anion Ratio Cl^+:SO_4^{2+}	Fe(II)-S		Fe(III)-S		Fe(III)-O		Fe(II)-S/ Fe(III)-S
	eV	Area%	eV	Area%	eV	Area%	
1:0	707.4	44	709.2	26	710.6	30	1.7
3:1	707.4	48	709.2	28	710.4	24	1.7
1:1	707.4	50	709.2	30	710.5	20	1.7
1:3	707.4	41	709.2	24	710.6	35	1.7

Note–Fe(2p) spectra are fit following the procedures in Nesbitt and Muir (1994) and Pratt, Muir, and Nesbitt (1994). Briefly, fit parameters are: Fe(II)-S–a primary peak coupled with two less intense peaks located 0.95 eV higher and lower than the primary peak. Fe(III)-S–contributions are characterized by a series of four peaks, progressively less intense occurring 1.75, 2.85, 3.85 and 4.75 eV above the primary Fe(II)-S peak. Peak area ratios relative to the first Fe(III)-S peak are 0.66, 0.35 and 0.15. Fe(III)-O–a sequence of four peaks progressively less intense towards higher binding energy, peak separations are 1.0, 1.2, and 1.4 eV, and peak intensities relative to the first are 0.95, 0.59, and 0.28.

example of Pratt, Muir, and Nesbitt (1994) and Mycroft, Nesbitt, and Pratt (1995), this portion of the spectrum is fit with the characteristic ferric multiplet sequence of four peaks beginning at 710.5 ± 0.1 eV (fig. 2; table 2). Comparison with reference binding energies in table 1 suggests this portion of the spectra results from a surface Fe(III)-oxyhydroxide.

Utilizing only Fe(II)-S and Fe(III)-O-OH components to fit the Fe(2$p_{3/2}$) spectra did not achieve a satisfactory result. Most notable was the poor fit in the region near 709 eV. Pratt, Nesbitt, and Muir (1994) were confronted with the same problem, and they obtained excellent fits, as do we here, using a Fe(III)-S species (fig. 2; table 2). Fe(III)-S species have been shown by Pratt, Muir, and Nesbitt (1994) to be present in pyrrhotite near-surfaces freshly fractured under high vacuum.

S(2p) spectra are dominated by a peak near 163.5 eV (fig. 2; table 3). Buckley and Woods (1985a), Tremes and others (1987), and Mycroft and others (1990) interpreted peaks in the energy range 162.8 to 163.8 eV to result from polysulfides. We interpret our peaks at 163.5 ± 0.1 eV (fig. 2, table 3) to be polysulfide. Pratt, Nesbitt, and Muir (1994) used a broad peak (FWHM = 2.2 eV) to fit the polysulfide component, arguing that the broadness of the fit peak resulted from the presence of a range of polysulfides (S_3^{2-} to S_7^{2-}). In contrast, all polysulfide contributions in these experiments were fit with FWHM = 1.1 eV (table 3), which suggests the presence of only one or two polysulfide species.

The low binding energy shoulder is best fit with two peaks at 161.5 ± 0.1 and 162.5 eV (table 3), indicating monosulfide and disulfide species (table 1). Pratt, Nesbitt, and Muir (1994) interpret peaks near 161.2 and 162.2 eV, respectively, to result from ferrous monosulfide and disulfide moieties in pyrrhotite. Disulfide is anticipated in pyrrhotite and originates from intersulfur octahedra bonds at vacant metal sites (Vaughan and Craig, 1978).

The highest binding energy component of the S(2*p*) spectra is best fit with a peak near 167.8 eV (table 3). Jones and others (1992) note that the sulfate peak on pyrrhotite surfaces is at 168.5 eV (table 1), and Wagner and others (1979) along with Turner and others (1980) list binding energies near 167.5 eV for inorganic thiosulfate species. We interpret the peak at 167.8 eV to be thiosulfate. A minor thiosulfate S-S component should occur toward the low binding energy portion of the spectra. The inclusion of a thiosulfate S-S component would be difficult to justify considering the the very weak intensity of the thiosulfate S-O component (<6 percent, table 3). Thiosulfates and other polythionate species have been observed by Steger and Desjardins (1978) and Steger (1982) during pyrrhotite oxidation.

TABLE 3

S(2$p_{3/2}$) peak fitting data. All peaks were fit with a FWHM of 1.1 eV

Anion Ratio $Cl^+:SO_4^{2+}$	S^{2-}		S_2^{2-}		S_n^{2-}		S_8		$S_2O_3^{2-}$		
	eV	Area %	eV	Area %	eV	Area %	eV	Area %	eV	Area %	$(S_2^{2-} + S_n^{2-} + S_8)/S^{2-}$
1:0	161.4	32	162.5	12	163.5	47	164.5	3	167.9	6	1.9
3:1	161.5	36	162.5	9	163.6	50			167.9	5	1.6
1:1	161.5	37	162.5	7	163.6	52			167.9	4	1.6
1:3	161.4	44	162.5	10	163.4	37	164.5	3	167.8	6	1.1

In two of the S(2*p*) spectra a constituent of elemental sulfur at 164.5 eV (table 3) is required to achieve good spectral fits. Buckley and Woods (1985a) note that sulfur is volatile in the vacuum of the XPS analytical chamber. Its detection in our sample suggests that the sulfur may be protected from sublimation by an overlayer, most likely the Fe(III)-oxyhydroxide.

The O(1*s*) spectra (fig. 2, table 4) are fit with a peak at 531.8 ± 0.2 eV which is attributed to hydroxyl oxygen. The low binding energy shoulder of each spectrum is best fit with a peak at 530.1 ± 0.1 eV (table 4) and is interpreted to originate from oxide oxygen (table 1). The high binding energy side of the O(1*s*) spectra requires a separate peak at 533.1 ± 0.1 eV (table 4)

TABLE 4

O(1s) peak fitting data. FWHM are constrained to the peak's natural line width and range from 1.2 for oxide on the 1:1 sample to 1.9 for attached water on the 1:3 sample

Anion Ratio $Cl^+:SO_4^{2+}$	O^{2-}		OH^-		H_2O		
	eV	Area%	eV	Area%	eV	Area%	O^{2-}/OH^-
1:0	530.0	18	531.6	65	533.0	17	0.28
3:1	530.0	12	532.0	70	533.0	18	0.17
1:1	530.2	13	531.9	61	533.3	26	0.21
1:3	530.2	12	531.9	47	533.2	41	0.26

which is attributed to oxygen of attached water. These interpretations are consistent with those of McIntyre and Zetaruk (1977), Harvey and Linton (1981), Mills and Sullivan (1983), Knipe and others (1995), and Junta-Rosso and Hochella (1996).

AES depth profiles.–Pyrrhotite surfaces leached with hydrochloric-sulfuric acid mixtures of 1:0, 3:1, 1:1, and 1:3 are shown in figure 3A, B, C and D respectively.

The hydrochloric acid experiment, $Cl:SO_4$ = 1:0, produced a sulfur-rich, iron depleted, alteration zone approx 120Å thick. There is little oxygen on the surface and effectively none in the alteration zone. Sulfur enrichment on pyrrhotite surfaces oxidized in air and leached in H_2SO_4 pH 3.0 has been noted elsewhere (Pratt, Muir, and Nesbitt, 1994; Pratt, Nesbitt, and Muir, 1994; Nesbitt and Pratt, 1995; Mycroft, Nesbitt, and Pratt, 1995) and has been interpreted to result from the diffusion of iron through structural vacancies to the pyrrhotite surface. A similar phenomenon is considered to have occurred here, with iron being removed from the surface by the HCl solution. It is apparent that although the HCl leachate is air-saturated, dissolved oxygen is not taken up on the surface in significant quantity. In fact the small amount seen on the surface (10 percent) may have resulted from slight contamination during transfer from the reaction vessel to the Auger instrument.

Pyrrhotites leached in solutions with the $Cl:SO_4$ = 3:1 and 1:1 have near-surfaces slightly enriched in sulfur relative to the pristine interior pyrrhotite. Oxygen concentrations are low, and the profiles are qualitatively similar to figure 3A. Although near-surface sulfur enrichment is less pronounced (fig. 3B,C), the enrichment probably results from removal of iron relative to sulfur. As well as displaying less sulfur enrichment, the alteration zone is only 30 to 40 Å thick (fig. 3B,C) compared with 120Å for the HCl-leached surface (fig. 3A).

Pyrrhotite leached in solutions with $Cl:SO_4$ = 1:3 contains Fe- and O-rich, S-depleted surface layers approx 20Å thick (fig. 3D). This compositional trend is not observed on the surfaces leached in solutions that contain greater amounts of Cl^-.

Beyond 20Å depth sulfur rises quickly to approx 60 atomic percent, iron decreases to approx 25 percent, and oxygen progressively decreases to background values (approx 5 atomic percent) near 450Å (fig. 3D). The S, Fe, and O atomic proportions in this zone are not representative of specific mineralogical compositions and indicate there probably are numerous "chemical species" in the zone. Iron is low by comparison with Fe-sulfide or Fe-oxyhydroxide minerals such as pyrite or goethite. The high sulfur content and pronounced cation deficiency is suggestive of polymerized sulfur species such as polysulfide or even elemental sulfur. This is in agreement with the S(2*p*) data and suggests that these species reside in the leached mineral near-surface. The detection of O within this zone indicates oxygenated species also occur. However, the nature of these species is not certain and based on the interpretations of the XPS results the O is most likely associated with polythionate and/or partially hydrated iron sulfur species.

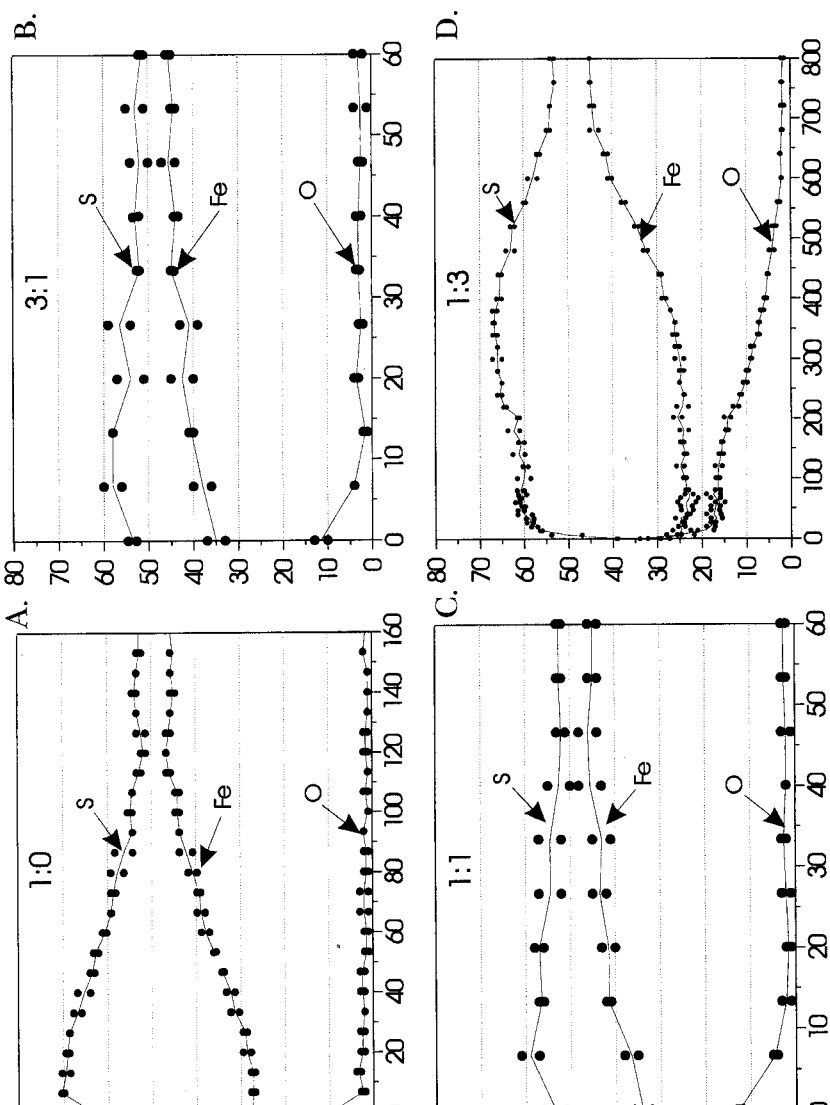

Fig. 3. AES depth profiles collected from pyrrhotite surfaces reacted in the various Cl^-:SO_4^{2-} acid mixtures, abscissa is depth in Ångstroms, and ordinate is atomic percent. Symbols (circles) represent analysis at two different surface points and the solid lines represent connected average values. See text for details.

Between 450 and 650Å Fe, S and O concentration trends are similar to those observed in the acid mixtures with lower sulfate concentrations. The near absence of oxygen within this zone may indicate that the dominate processes involve iron diffusion and sulfur polymerization. The absence of oxygen in the 450 to 650Å range indicates that this zone is on average less oxidized than the shallower zones. The deepest zone (greater than 650-700Å) reflects pristine pyrrhotite composition.

Solution chemistry.–As shown in figure 4A, sulfate and iron are present in solution after 15 mins leaching, with sulfate the more abundant. Sulfate content does not increase with continued reaction. The sulfate concentration trend can be explained by the initially rapid dissolution of soluble iron sulfate salts. Pratt, Muir, and Nesbitt (1994) Mycroft, Nesbitt, and Pratt (1995), Buckley and Woods (1985b) report that sulfate will form rapidly on pyrrhotite surfaces exposed to air. From this it would be reasonable to suggest that sulfate initially occurs as surface resident salts which form during sample preparation. The concentration trend indicates that sulfate release over the first six hrs of reaction is a one-time event, is the first species detected, and is most rapid of the leaching reactions.

Iron concentrations plotted against time yield curved trends (fig. 4A) but plotted against the square root of time yield linear trends over much of the early leaching period (fig. 4B). Deviation from the linear trend is observed after about 4 hrs (fig. 4B, $\sqrt{\text{time}} = 16$), and a plateau exists near 0.065 millimoles of iron released. The linear trend defined by results of the first 4 hrs suggests that diffusion controls the iron leaching rate.

As with the 25°C data, the 35°C Fe(aq) data plotted against the square root of time yield linear trends during the early stages of dissolution (up to 2 hrs; $\sqrt{t} = 11$) (fig. 5). After approx 2 to 3 hrs of leaching ($\sqrt{t} = 13$) the Fe_t(aq) concentrations plot below the extrapolated linear trend, and a maximum in Fe(aq) concentration is found to occur at approx 4 to 5 hrs (fig. 5, $\sqrt{t} = 16$-17). The maximum is followed by a decline to a value near 0.048 millimoles of Fe(aq). In closed systems, such as here, concentration increases are often due to dissolution or desorption/exchange, and concentration decreases to precipitation or adsorption/exchange. The observation that iron concentrations go through a maximum indicates that Fe(aq) removal rates have approached or exceeded release rates. The sink for iron in this study would be the yellow-to-rust colored colloidal suspension identified as lepidochrosite (γFeOOH) by XRD. At approx 17 to 20 $min^{1/2}$ apparently steady state conditions are attained.

The five experiments at 25° and 35°C contain different proportions of chloride and sulfate in solution, yet the slopes defined by the data for each experiment are essentially the same (table 5). Either both anions have precisely the same effect on leach rates for iron, or they have no effect. Furthermore, Fe(III)-oxyhydroxide coatings form on pyrrhotite surfaces leached in pH 3.0 H_2SO_4 (Pratt, Nesbitt, and Muir, 1994), whereas Fe-polysulfide species are found on surfaces leached in solutions containing Cl^-. Although the near-surface regions of leached pyrrhotite are compositionally different, these compositionally different surfaces have no effect on the leach

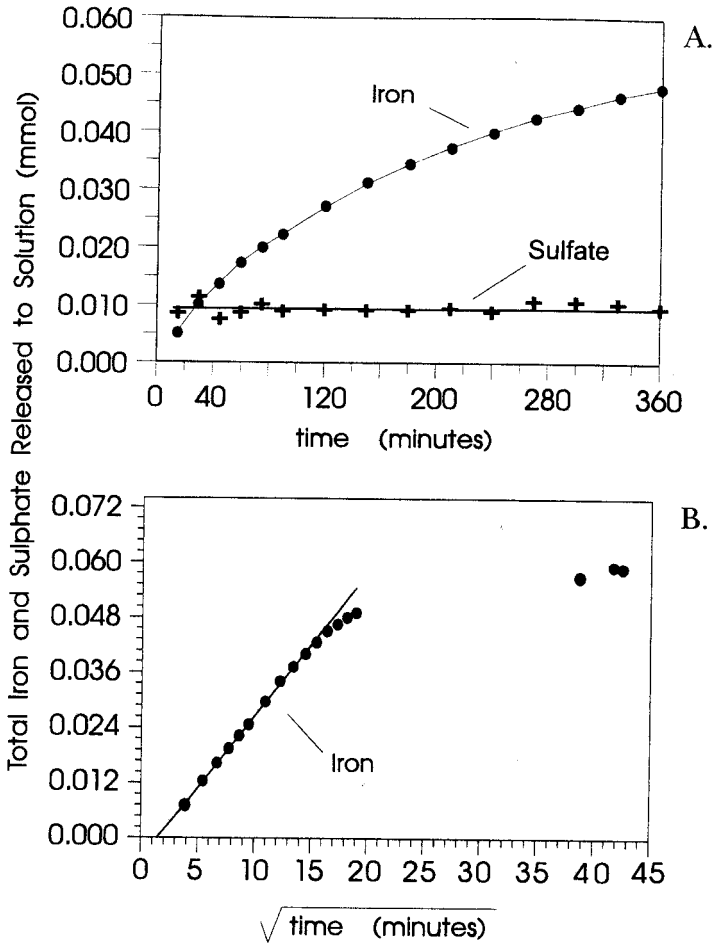

Fig. 4. Representative plots illustrating concentration trends for ions in solution (25°C); (A) acid mixture with $Cl^-:SO_4^{2-}$ = 1:0 showing iron and sulfate concentrations plotted as function of time for the first 6 hrs of reaction; (B) acid mixture with $Cl^-:SO_4^{2-}$ = 0:1 showing iron concentrations plotted as a function to the square root of time over the duration of the experiment. The presented iron and sulfate data have been corrected for the volume of solution removed for analysis.

rate of these experiments. From these observations we conclude that the *same process controls the rate of release of iron to solution* in all these experiments, that chloride and sulfate have no apparent effect on leach rates, and that the composition of the altered layer on the pyrrhotite grains has no effect on leach rates, at least over the duration of the experiments.

The pH of leachates, at both temperatures, is observed to increase from pH 3.0 to approx pH 5.0 (fig. 6). This trend is particularly accentuated with

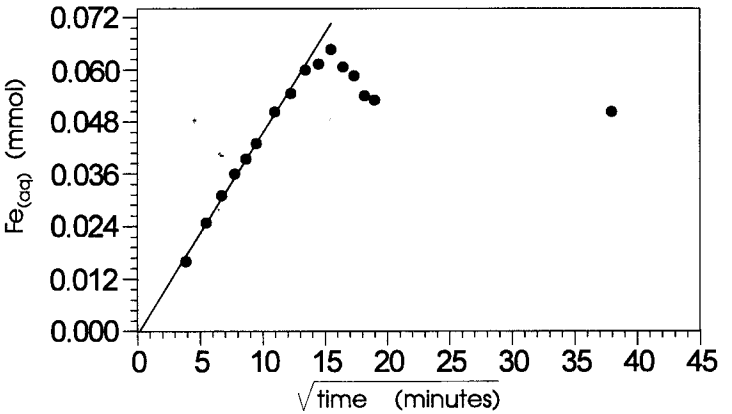

Fig. 5. Representative plot showing the dissolved iron concentration trend in solution at 35°C. Data from acid mixture batch experiment using $Cl^-:SO_4^{2-} = 3:1$.

the 35°C data. The increase in pH indicates that $H^+(aq)$ is consumed as the reactions proceed. The attainment of maximum pH values appears to coincide with steady state conditions for iron. Since this correlation occurs for all experimental solutions, it would appear that the correlation is unlikely to be coincidental; rather consumption and production of $H^+(aq)$ are equal after pH = 5.0 is achieved. The H^+ production reaction may be precipitation of lepidochrosite as colloids, as discussed subsequently.

DISCUSSION

Surface processes.–The leaching of pyrrhotite by air-saturated HCl solution (fig. 3A) causes iron from the bulk pyrrhotite to diffuse to the surface where it is taken into solution. Sulfur remains in the solid to produce a residual sulfur-enriched alteration zone dominated by polysulfide species. The properties of the interface and nature of the solutes apparently inhibit

TABLE 5

Experimental rate constants ($2k_p$) obtained from the measured Fe concentrations in solution, experimental rate constants corrected for surface area ($2k_{ps}$) and activation energies (E_a) determined from the measured iron concentrations

	25°C		35°C		
Acid	$2k_p$ (mmol)	$2k_{ps}$ (mmol $min^{-1/2}$)	$2k_p$ (mmol)	$2k_{ps}$ (mmol $min^{-1/2}$)	E_a kJ/mole
1:0	3.04×10^{-3}	8.69×10^{-6}	4.23×10^{-3}	1.21×10^{-5}	25
3:1	2.97×10^{-3}	8.49×10^{-6}	4.14×10^{-3}	1.18×10^{-5}	26
1:1	2.91×10^{-3}	8.31×10^{-6}	4.03×10^{-3}	1.15×10^{-5}	25
1:3	3.25×10^{-3}	9.28×10^{-6}	4.60×10^{-3}	1.31×10^{-5}	26
0:1	3.09×10^{-3}	8.83×10^{-6}	4.23×10^{-3}	1.21×10^{-5}	24

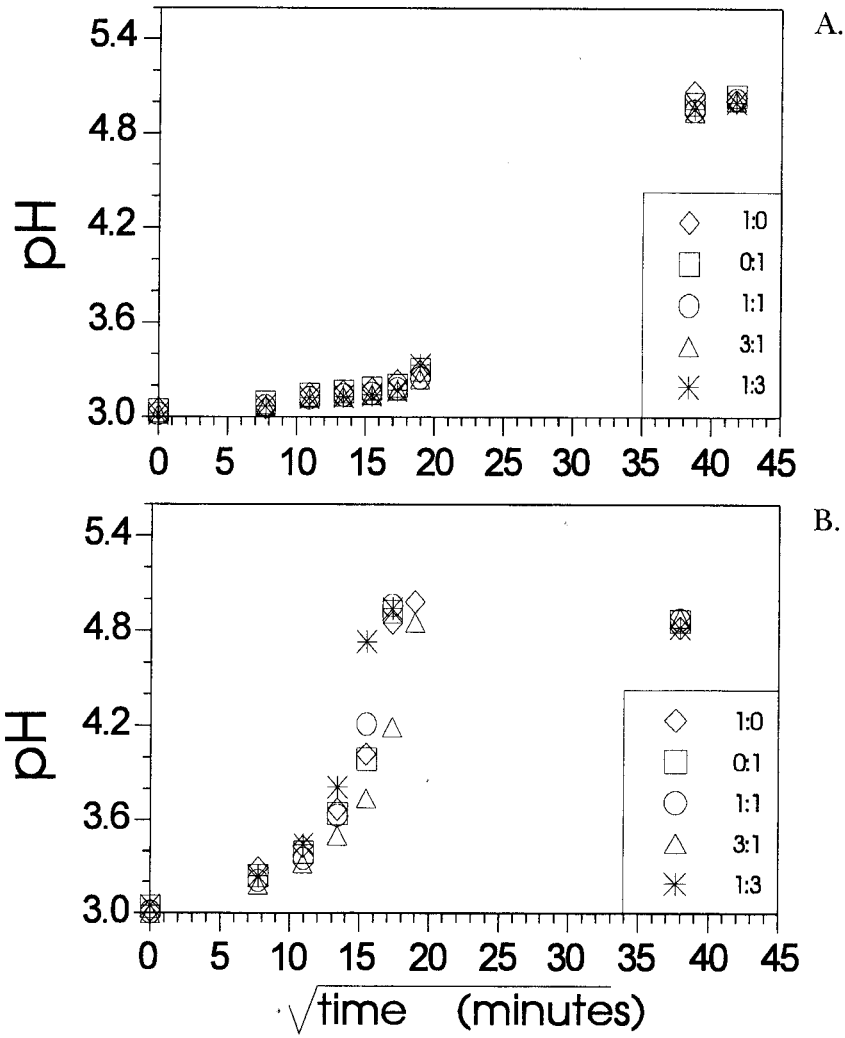

Fig. 6. Measured pH values for leaching batch experiments at 25°C (A) and 35°C (B). The pH is presented as a function of the square-root of time solely for convenient comparison with dissolved iron values, no chemical processes are implied.

oxygen uptake onto the solid surface and its consequent diffusion into the sulfur-rich alteration zone. These same processes affect pyrrhotite leached by solutions containing HCl and H_2SO_4 in the ratios 3:1 and 1:1.

Markedly different compositional profiles are produced by leaching with a pH 3.0 solution containing a 1:3 mixture of HCl and H_2SO_4. Iron from pyrrhotite diffuses to the solid/solution interface. Once at the surface, iron is

oxidized and deposited at the interface as Fe(III)-oxyhydroxides, thus an oxyhydroxide layer is "built" outward from the original surface. This process leaves the surface rich in oxygen species. The sulfur enriched zone beneath the Fe(III)-oxyhydroxide layer contains appreciable oxygen (fig. 3D). The elevated oxygen levels and the continual decrease of oxygen with depth indicate that oxygen, originally within the solution, has penetrated the sulfur enriched sublayer, probably by diffusion through vacancies in the pyrrhotite lattice. The actual species being transported to the subsurface is uncertain. If the species is hydroxide, then a process involving counter diffusion of OH^- into the sulfur-rich zone and iron diffusion from the interior to the surface may be occurring.

All leaching solutions had the same initial pH but variable Cl^- to SO_4^{2-} ratios, yet compositional profiles, and alteration processes differ depending upon the Cl^- to SO_4^{2-} ratio in solution. The major difference between the profiles is that oxygen is dramatically reduced on the surface and interior of the solid where chloride is abundant. With sulfate dominant, oxygen is the most abundant element at the solid surface, and it penetrates a few hundred Ångstroms into the sulfur-rich underlayer. Clearly, chloride prohibits the uptake of reactive oxygen-bearing species onto the solid surface and, in doing so, prohibits diffusion of oxygen into the subsurface.

XPS S(2*p*) spectra further emphasize the influence chloride. The most striking change to the sulfur spectra is the proportional decrease in monosulfide at the expense of disulfide (S_2^{2-}), polysulfides (S_n^{2-}), and S°. The last three species are referred to subsequently as multimeric sulfur species (S_n where n = 2 to 8). The ratio of multimeric to monosulfide changes systematically from near 2:1 to near 1:1, as the proportion of chloride is decreased in the leaching solutions (table 3). The change in ratio may be related to the ability of chloride to inhibit both the uptake of oxygen onto the solid surface and the diffusion of oxygen species into the interior of the solid (table 3). With limited supply of oxidant at the surface, intermediate oxidation products are produced rather than oxygen sulfur species such as thiosulfate.

The ratio of ferric sulfide (Fe[III]-S) to ferrous sulfide (Fe[II]-S) is 0.48:1.0 for pristine pyrrhotite, and with air oxidation the ratio decreased appreciably (Pratt, Muir, and Nesbitt, 1994). The decrease was interpreted to indicate a greater reactivity of Fe(III)-S surface species towards molecular oxygen (oxidant) than Fe(II)-S species, where Fe(III)-bonded to sulfur was preferentially destroyed to produce Fe(III)-oxyhydroxides. The ratios observed here are 1.7:1 regardless of the proportion of chloride in solution. Leaching by these air-saturated solutions produces the opposite result to air-oxidation; there is exceptional enhancement of the Fe(III)-S species over Fe(II)-S. A major difference between the two experiments is the possibility to remove surface constituents to aqueous solution. We suggest that the enhanced Fe(III)-S signal results from preferential removal of iron(II) from the surface to solution without oxidizing sulfide to its most stable form sulfate. Intermediate oxidation products of sulfide, primarily disulfides and polysulfides, accumulate in the near-surface rather than oxygen sulfur species. We hypothesize that the sulfur-rich zone of the near-surface results from incongruent dissolu-

tion of pyrrhotite coupled with partial oxidation of monosulfide to multimeric species primarily.

The O(1*s*) data (fig. 2, table 4) indicate the presence of O^{2-} (oxide oxygen), OH^- (hydroxide), and H_2O (attached water), and the Fe(2*p*) data (table 2) indicate that the oxygen-bearing species are present as Fe(III)-oxyhydroxide species primarily. The small amount of thiosulfate detected (fig. 2, table 3) implies a small contribution from oxygen bonded to sulfur (thiosulfates). The O^{2-}:OH^- ratio for all experiments show an excess of hydroxide relative to oxide (table 4), whereas for lepidochrosite or goethite the ratio is 1:1. These results suggest that species forming at the surface are most likely a mixture of oxyhydroxides and hydroxides rather than a distinct iron phase.

Solution processes.–Aqueous iron concentrations plotted against time show parabolic curves and, when plotted against the square root of time, yield linear trends for the first few hours for all experiments. The parabolic release rate may be the result of a variety of processes, most important of which may be variation in grain size (Talman and Nesbitt, 1988). The parabolic rate law, however, accurately describes all results for the first few hours of leaching, and as discussed subsequently the numerous experiments yield remarkably consistent apparent activation energies (table 5). Subsequent, more detailed experiments may demonstrate that surface reactions are important in controlling reaction rates. However, in the absence of additional evidence, the process controlling iron release to solution during the initial stage of leaching is here considered to be diffusion.

Apparent activation energies (E_a) calculated from the experimental rate constants listed in table 5 are near 25 kJ/mole. E_a of this magnitude are more representative of ion diffusion through a solution than through a solid (Orr and Butler, 1935; Ahonen and Tuovinen, 1992). For comparison the E_a for iron diffusion along the c-axis of monoclinic pyrrhotite at 254°C is 90 kJ/mole (Condit and others, 1974). The presence of solution diffusion kinetics in our study is not unexpected. Lerman (1979) notes that in closed system leaching experiments the initial stages of mineral dissolution are generally controlled by solution diffusion processes.

Insight into processes involving hydrogen ions is obtained by comparing the amounts of iron released to and hydrogen removed from solution. The slopes of the first five points on figure 7A (first 5 hrs of leaching) are close to 2.00, indicating that two moles of H^+ are consumed for every mole of iron released to solution. The anion-cation relationship suggests charge balance is maintained by exchange of H^+ and Fe^{2+} between the bulk solution and the solid. If so, the reaction is effectively an exchange reaction:

$$FeS_{(surface)} + 2H^+(aq) \Leftrightarrow H_2S_{(surface)} + Fe^{2+}(aq), \quad (1)$$

where FeS is a surface species (the Fe(II)-S component of Fe_7S_8). H_2S appears to be a solid species as only a minute amount of gas is produced during the experiments. The H_2S species is most likely ephemeral and probably forms in the near-surface of the leached pyrrhotite as a consequence of exchange.

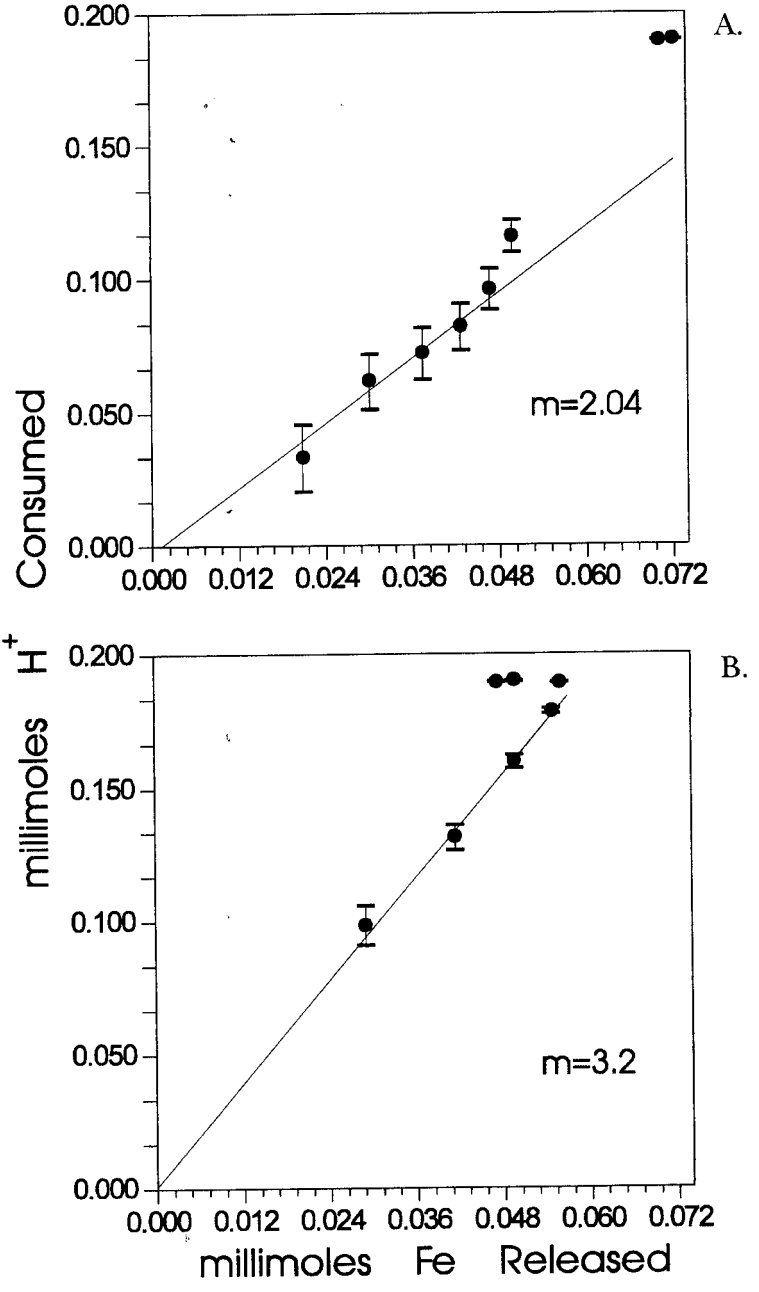

Fig. 7. Diagrams depicting the relationship between the amount of hydrogen ions removed from solution and the amount of iron released to solution: (A) 25°C, acid mixture with Cl^-: SO_4^{2-} = 3:1; and (B) 35°C, acid mixture with Cl^-:SO_4^{2-} = 1:0. The plotted hydrogen and iron values have been corrected for the volume of solution removed for analysis. Hydrogen values are plotted with an absolute error in measurement of 0.03 pH units.

The charge balance between H^+ and Fe(aq) suggests that Fe^{2+} is the primary ion released to solution.

The fate of H^+ after uptake onto active exchange or sorption sites is unknown because its concentration and distribution cannot be determined by our surface analytical techniques (XPS, AES). There are, however, a large number of structural vacancies in pyrrhotite, hence some H^+ likely diffuses to the interior of pyrrhotite due to the chemical potential gradient between surface and interior. In turn, H^+ may promote migration of iron to the surface by acting as the counter ion for iron diffusion. By considering the charge and "size" of the ionic species, it is likely iron controls the rate of migration of H^+ from the surface to the interior of the solid, possibly through coupled (counterion) diffusion. If so, then Fe^{2+}-H^+ exchange (Rxn. 1) should be regarded as a bulk volume exchange rather than a surface exchange process. The relationship between surface area to reaction rate then becomes somewhat ambiguous.

Identification of γFeOOH as an oxidation product provides significant insight into subsequent processes occurring during the batch experiments. γFeOOH usually develops in systems dominated by ferrous iron and is formed by an oxidative/hydrolytic mechanism (Ross and Wang, 1982; Schwertmann and Cornell, 1991). Throughout these experiments Fe^{2+}(aq) is the dominant aqueous iron species, a prime requirement for γFeOOH formation. Deviation from linear concentration trends at 25°C occur after 4 to 6 hrs of dissolution (fig. 4B). The deviation of trends can be accounted for by the oxidation of ferrous iron to ferric iron in the aqueous phase. As pH within the solutions increases saturation with Fe(III)-oxyhydroxides is approached and exceeded, resulting in precipitation. Reactions describing Fe^{2+} oxidation, H^+ consumption, and Fe(III)-oxyhydroxide production are:

$$2Fe^{2+} + 1/2O_2 + 2H^+ \Leftrightarrow 2Fe^{3+} + H_2O \quad (2)$$

$$Fe^{3+} + 2H_2O \Leftrightarrow \gamma FeOOH + 3H^+ \quad (3)$$

by summing the H^+ in reactions (1) and (2) a 3 to 1 relationship emerges between H^+ consumption and Fe^{2+} release to solution. A 3 to 1 relationship is observed for the 35°C data (fig. 7B) and may be an indication of the occurrence of reaction (2) during the batch experiments. Furthermore, deviation from the 2 to 1 relationship for the sixth 25°C data point (fig. 7A) may also result from the onset of dissolved ferrous oxidation.

According to Schwertmann and Cornell (1991) γFeOOH only forms within a pH 5 to 7 range. If pH is above 7 in a ferrous dominated system, αFeOOH forms (Schwertmann and Cornell, 1991). Once pH 5 is attained in our experiments, it would appear hydrolysis of ferric iron proceeds and γFeOOH forms following reaction (3). An implication of reaction (3) is that the system is self buffering with regard to pH, as long as dissolution and precipitation proceed at a commensurate rates.

A second product of reaction identified by XRD is elemental sulfur. Its development may be related to processes occurring at the mineral surface. As shown by Buckley and Woods (1985b) and Pratt, Muir, and Nesbitt (1994) pyrrhotite contains monosulfide (S^{2-}) primarily, but as previously empha-

sized, monosulfide of the near-surface is oxidized to polysulfides and elemental sulfur during leaching. A reaction compatible with these observations is:

$$FeS_{surface} + 1/2O_2(aq) + 2H^+(aq) = Fe^{2+}(aq) + S^\circ + H_2O. \quad (4)$$

where FeS is a surface species (the Fe(II)-S component of Fe_7S_8). Reaction (4) incorporates the exchange reaction (1) with the oxidation reaction of monosulfide to S°. The oxidized sulfur may be found in the leached layer of pyrrhotite as polysulfide or as elemental sulfur.

An additional reaction probably occurs in the leached near-surface zone of pyrrhotite, as it does during oxidation of pyrrhotite in air (Mycroft, Nesbitt, and Pratt, 1995). As noted previously, iron(II) of pyrrhotite may be oxidized according to:

$$FeS + 3/2O_2(aq) + 1/2H_2O = FeOOH + S^\circ \quad (5)$$

where FeS is again a proxy for pyrrhotite, and S° is incorporated into polysulfides and elemental sulfur of the sulfur-rich altered layer.

Implications for acid mine drainage.–These results suggest that chloride may have a significant role in the generation of acid mine drainage. For example, the integrity of reaction passivating overlayers of oxide, hydroxide and sulfate species on sulfide minerals are markedly compromised by desiccation and spalling processes during wet-dry or freeze-thaw cycles (Pratt, Nesbitt, and Muir, 1994). The presence of chloride in pore solutions may inhibit regeneration of these passivating layers on exposed sulfide surfaces and prolong exposure to and reaction with oxidizing solutions. There is, therefore, the potential to produce, very rapidly, acidic mine drainage through the oxidation of sulfur and subsequent formation of sulfate. Furthermore, addition of Cl^--bearing solutions (dissolved chloride salts or HCl), such as used for processing of some ores (Craigen and others, 1990; Collins and Flett, 1990), to mine tailings or waste rock piles may limit development of Fe(III)-oxyhydroxide surface coatings on recently stored gangue sulfide minerals and potentially lead to prolonged production of acidic drainage.

CONCLUSIONS

In solutions where the concentration of chloride is dominant over sulfate, pyrrhotite surfaces are virtually devoid of oxygenated species. Surfaces tend to be depleted in iron and enriched in sulfur, with polysulfide species dominating. When sulfate concentrations are in excess of chloride the abundance of oxygen species at the surface increases, and penetration of oxygen species into the solid occurs. The results of this study demonstrate that chloride does not allow Fe(III)-oxyhydroxides to accumulate in appreciable amounts on the altered pyrrhotite surface.

Leaching experiments show that one of the earliest stages of pyrrhotite dissolution involves the rapid release of sulfate. This stage is followed by the release of iron to solution via a diffusion controlled process characterized by H^+ consuming reactions. Variation in solution $Cl:SO_4$ ratios and the nature

of leached surfaces do not appear to have any significant effect on the release rates for iron.

ACKNOWLEDGMENTS

The authors wish to thank Dr. N. S. McIntyre of Surface Science Western for generously sharing the facilities and his expertise with us. We also thank the following people for their assistance and suggestions Dr. J. R. Mycroft, Dr. I. J. Muir, Mr. G. Matsu, Mr. G. Hoffmann (AA analyses), and Mr. H. P. Wagner (IC analyses). Comments and criticisms from three anonymous referees greatly improved the manuscript. These studies were supported through grants from the National Sciences and Engineering Research Council of Canada and the Mine Environment Neutral Drainage program (MEND, CANMET, Ottawa, Canada). A.R.P. received additional support in the form of an Ontario Graduate Scholarship.

REFERENCES

Al, T. A., Blowes, D. W., and Jambor, J. L., 1994, A geochemical study of the main tailing impoundment at the Falconbridge Limited, Kidd Creek Division Metallurgical site, Timmins, Ontario, *in* Jambor, J. L., and Blowes, D. W., editors, Environmental Geochemistry of Sulfide Mine-Wastes: Mineralogical Association of Canada, v 22, p. 333–364.

Ahonen, L., and Tuovinen, O. H., 1992, Bacterial oxidation of sulfide minerals in column leaching experiments at suboptimal temperatures: Applied Environmental Microbiology, v. 58, p. 600–606.

Bhatti, T. M., Bigham, J. M., Carlson, L., and Touvinen, O. H., 1993, Mineral products of pyrrhotite oxidation by *Thiobacillus ferrooxidans:* Applied Environmental Microbiology, v. 59, p. 1984–1990.

Blowes, D. W., and Jambor, J. L., 1990, The pore-water geochemistry and the mineralogy of the vadose zone of sulfide tailings, Waite Amulet, Quebec, Canada: Applied Geochemistry, v. 5, p. 327–346.

Buckley, A. N., and Woods, R., 1985a, X-ray photoelectron spectroscopy of oxidized pyrrhotite surfaces. II: Exposure to aqueous solutions: Applied Surface Science v. 20, p. 472–480.

—— 1985b, X-ray photoelectron spectroscopy of oxidized pyrrhotite surfaces. I: Exposure to air: Applied Surface Science, v. 22/23, p. 280–287.

Caboi, R., Cidu, R., Fanfani, L., Massoli Noveeli, R., and Zuddas, P., 1992, Metal contamination of stream waters from former mining activity. *in* Kharaka, Y. K. and Maest, A. S., editors, Water-Rock Interaction: Rotterdam, Balkema, p. 367–370.

Carlson, T. A., 1975, Photoelectron and Auger Spectroscopy: New York, Plenum Press, 417 p.

Collins, D. N., and Flett, D. S., 1990, Role of chloride hydrometallurgy in processing of complex (massive) sulfide ores. *in* Gray, P. M. J., Bowyer, G. J., Castle, J. F., Vaughan, D. J., and Warner, N. A., editors, Sulfide Deposits their origin and processing: London, The Institution of Mining and Metallurgy, p. 233–254.

Condit, R. H., Hobbins, R. R., and Birchenall, C. E., 1974, Self-diffusion of iron and sulfur in ferrus sulfide: Oxidation of Metals v. 8, p. 409–455.

Craigen, W. J. S., Kelly, F. J., Bell, D. H., and Wells, J. A., 1990, Evaluation of the CANMET ferric chloride lead (FCL) process for treatment of complex base-metal sulfide ores. *in* Gray, P. M. J., Bowyer, G. J., Castle, J. F., Vaughan, D. J., and Warner, N. A., editors, Sulfide Deposits their origin and processing: London, The Institution of Mining and Metallurgy, p. 254–270.

Gupta, R. P., and Sen, S. K., 1974, Calculation of Multiplet Structure of Core *p*-vacancy Levels. I: Physical Review B. v. 10, no. 1, p. 71–79.

—— 1975, Caculation of Multiplet Structure of Core *p*-vacancy Levels. II: Physical Review B. v. 12, No. 1, p. 15–19.

Harvey, D. T., and Linton, R. W., 1981, Chemical Characterization of Hydrous Ferric Oxides by X-ray Photoelectron Spectroscopy: Analytical Chemistry, v. 53, p. 1648–1688.

Hochella, M. F., Jr., 1988, Auger electron and X-ray photoelectron spectroscopies, *in* F. C. Hawthorne, Spectroscopic Methods in Mineralogy and Geology: Reviews in Mineralogy, v. 23, p. 573–638.

Hutchinson, I. P. G., and Ellison, R. D., 1992, Mine Waste Management: Chelsea, Michigan, Lewis Publishers Inc., 654 p.

Hyland, M. M., and Bancroft, G. M., 1989, An XPS study of gold deposition at low temperatures on sulfide minerals: Reducing agents: Geochimica et Cosmochimica Acta, v. 53, p. 367–372.

Jones, C. F., Lecount, S., Smart, R. St. C., and White, T., 1992, Compositional and structural alteration of pyrrhotite surfaces in solution: XPS and XRD studies: Applied Surface Science, v. 55, p. 65–85.
Junta-Rosso, J. L., and Hochella, M. F. Jr., 1996, The chemistry of hematite {001} surfaces: Geochimica et Cosmochimica Acta, v. 60, p. 305–314.
Knipe, S. W., Mycroft, J. R., Pratt, A. R., Nesbitt, H. W., and Bancroft, G. M., 1995, X-ray photoelectron spectroscopic study of water adsorption on iron sulfide minerals: Geochimica et Cosmochimica Acta, v. 59, p. 1079–1090.
Lerman, A., 1979, Geochemical processes water and sediment environments: New York, John Wiley & Sons, 481 p.
McIntyre, N. S., and Zetaruk, D. G., 1977, X-ray Photoelectron Spectroscopic Studies of Iron Oxides: Analytical Chemistry, v. 49, p. 1521–1529.
Mills, P., and Sullivan, J. L., 1983, A study of the core level electrons in iron and its three oxides by means of photoelectron spectroscopy: Journal of Physics D: Applied Physics: v. 16, p. 723–732.
Mycroft, J. R., Bancroft, G. M., McIntyre, N. S., Lorimer, J. W., and Hill, I. R., 1990, Detection of sulfur and polysulfides on electrochemically oxidized pyrite surfaces by X-ray photoelectron spectroscopy and Raman spectroscopy: Journal of Electroanalytical Chemistry, v. 292, p. 139–152.
Mycroft, J. R., Nesbitt, H. W., and Pratt, A. R., 1995, X-ray photoelectron and Auger electron spectroscopy of air oxidized pyrrhotite: Distribution of oxidized species with depth: Geochimica et Cosmochimica Acta, v. 59, p. 721–733.
Nesbitt, H. W., and Muir, I. J., 1994, X-ray photoelectron spectroscopic study of a pristine pyrite surface reacted with water vapour and air: Geochimica et Cosmochimica Acta, v. 58, p. 4667–4679.
Nesbitt, H. W., and Pratt, A. R., 1995, Applications of Auger electron spectroscopy to geochemistry: The Canadian Mineralogist, v. 33, no. 2, p. 243–259.
Nicholson, R. N., and Scharer, J. M., 1994, Laboratory studies of pyrrhotite oxidation kinetics: *in* Alpers, C. N., and Blowes, D. W., editors, Environmental geochemistry of sulfide oxidation, American Chemical Society Symposium Series v. 550, p. 14–30.
Orr, W. J. C., and Butler, J. A. V., 1935, The rate of diffusion of deuterium hydroxide in water: Transactions of the Chemical Society, p. 1273–1277.
Physical Electronics, 1976, Handbook of Auger Electron Spectroscopy (Technical supplement): Eden Praire, Minnesota, Perkin Elmer (Physical Electronics), p. 51.
Pratt, A. R., Muir, I. J., and Nesbitt, H. W., 1994, X-ray photoelectron and Auger electron spectroscopic studies of pyrrhotite and mechanism of Air Oxidation: Geochimica et Cosmochimica Acta, v. 58, p. 827–841.
Pratt, A. R., Nesbitt, H. W., and Muir, I. J., 1994, Generation of Acids in Mine Waste Waters: Oxidative leaching of pyrrhotite in dilute H_2SO_4 solutions (pH 3.0): Geochimica et Cosmochimica Acta, v. 58, p. 5147–5159.
Ritcey, G. M., 1989, Tailings Management, Problems and solutions in the mining industry: Amsterdam, Elsevier, 970 p.
Ross, G. J., and Wang, C., 1982, Lepidocrocite in a calcareous, well-drained soil: Clays and Clay Minerals, v. 30, p. 394–396.
Shirley, D. A., 1972, High-resolution X-ray photoemission spectrum of the valence bands of gold: Physical Review B, v. 5, p. 4709–4714.
Schwertmann, U., and Cornell, R. M., 1991, Iron Oxides in the Laboratory: VCH, Weinheim, 137 p.
Steger, H. F., 1982, Oxidation of sulfide minerals VII. Effect of temperature and relative humidity on the oxidation of pyrrhotite: Chemical Geology, v. 35, p. 281–295.
Steger, H. F., and Desjardins, L. E., 1978, Oxidation of sulfide minerals, 4. Pyrite, chalcopyrite and pyrrhotite: Chemical Geology, v. 23, p. 225–237.
Talman, S. J., and Nesbitt, H. W., 1988, Dissolution of populations of ultrafine grains with applications to feldspars: Geochimica et Cosmochimica Acta, v. 52, p. 1467–1471.
Tones, P. I., 1982, Limnological and fisheries investigation of the flooded open pit at the Gunnar uranium mine: Saskatoon, Canada, Saskatchewan Research Council, Publication C-805-10-E-82.
Tremes, S. C., Buckley, A. N., and Gillard, R. D., 1987, 2p Electron binding energies for sulfur atoms in metal polysulfides: Inorganica Chimica Acta. v. 126, p. 79–82.
Van der Heide, H., Hemmel, R., Van Bruggen, C. F., and Haas, C., 1980, X-ray photoelectron spectra of 3d transition metal pyrites: Journal of Solid State Chemistry, v. 33, p. 17–25.
Wagner, C. D., Riggs, W. M., Davis, L. E., Moulder, J. F., and Mailenberg, G. M., 1979, Handbook of X-ray Photoelectron Spectroscopy: Eden Prairie, Minnesota, Perkin-Elmer, (Physical Electronics), 189 p.